Orientation and Structure Development in Poly(trimethylene terephthalate) Tensile Drawing

Hoe H. Chuah†

Shell Chemical Company, Houston, Texas 77251-1380

Received February 22, 2001; Revised Manuscript Received July 20, 2001

ABSTRACT: Tensile drawing of poly(trimethylene terephthalate) (PTT) was studied at room temperature, 35, 50, and 75 °C. Instead of a typical increase in draw ratio with increasing temperature, the PTT draw ratio first increased, went through a maximum, and decreased; all occurred within a narrow range of temperature between T_g and T_g + 30 °C. This unusual drawing behavior was due to the onset of cold crystallization during hot drawing. The fast cold crystallization rate could become dominating at high draw temperature, impeding PTT drawability to the extent that it caused in situ ductile−brittle transition and draw failure. The crystal orientation function, f_c, measured with wide-angle X-ray diffraction (WAXD), increased rapidly with draw, and saturated at $f_c \approx 0.96$. Four IR vibration modes at 933, 1037, 1358, and 1505 cm^{-1} wavenumbers were found to be sensitive to draw for dichroic ratio characterization. By combining WAXD and IR orientation measurements, transition moment vectors of three crystalline 933, 1358, and 1505 cm^{-1} vibrations were found to make 54°, 29°, and 45° angles to the *c*-chain axis. The 933 and 811 cm^{-1} CH_2 rocking modes were used to estimate changes in PTT's methylene gauche conformation in drawing. The gauche content increased with increasing draw ratio; however, it is a unique function of the polymer's final crystallinity obtained through a combination of strain-induced and cold crystallizations irrespective of the draw temperatures.

Introduction

Poly(trimethylene terephthalate) (PTT) is an odd-numbered aromatic polyester with a chemical structure shown in Figure 1. Compared to the two familiar "even-numbered" poly(ethylene terephthalate) (PET) and poly(butylene terephthalate) (PBT) with two and four methylene units, respectively, there are very few studies on PTT because the polymer was not readily available until recently.[1]

PTT has some unusual mechanical properties. Ward et al.[2] were among the first to systematically study PTT fiber properties and deformation. They found PTT to have very good tensile elastic recovery. It was ranked in the unexpected descending order of PTT > PBT > PET. In a follow-up study, PTT fiber was deformed in situ in a wide-angle X-ray diffractometer, and changes in the fiber period *d*-spacing along the *c*-axis were measured as a function of strain.[3] The fiber period was found to increase immediately and in direct proportion to the applied macroscopic strain up to 4% before deviating from affine deformation. Furthermore, the deformation was reversible below this critical strain. This microscopic reversible crystal chain deformation was attributed to PTT's three methylene units arranged in a highly contracted and a very compliant gauche−gauche conformation.[4,5] The chain contraction is even more pronounced than PBT's gauche−trans−gauche conformation.[6] Since the initial deformation primarily involved torsional rotation of the gauche methylene C−C bonds, the force needed was only a fraction of that for bond stretching of trans conformers. Thus, polymers with helical chain conformation have low crystal moduli, about 20% of the moduli if the chains were in all-trans conformations.[7] Indeed, Nakamae et al.[8] found PTT to have a very low X-ray crystal modulus of 2.59 GPa compared to 107 GPa of PET.[9]

† E-mail: hoe@shellus.com.

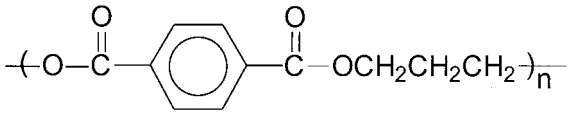

Figure 1. PTT chemical structure.

In this article we report PTT tensile drawing behavior. Orientation and structural development were studied by wide-angle X-ray diffraction (WAXD), infrared (IR) dichroism, and density and thermal analysis.

Experimental Section

Sample Preparation and Tensile Drawing. PTT (M_n = 17 300, M_w = 35 200, Shell Chemical Company) was compression-molded into ~0.7 mm thick film at 250 °C and quenched in ice water. American Society of Testing Methods ASTM-D638 type V dog-bone samples were die-cut from the film. Stress−strain curves were measured with an Instron tensile machine, model 1122, equipped with a circulating hot air chamber at room temperature, 35, 50, and 75 °C, a range of temperatures just below and above PTT's glass transition of 45 °C. The drawing rate was 2.54 cm/min. PTT samples were also drawn at 35, 50, and 75 °C to various draw ratios for structure development studies. The draw ratio was measured from the change in lengths of spacings marked at 1 cm interval.

Wide-Angle X-ray Crystal Orientation Function Measurements. The Herman crystal orientation function, f_c, was measured by azimuthal scanning of the equatorial 010 reflection at $2\theta = 15.4°$ with a Rigaku Denkki wide-angle X-ray diffractomer equipped with a goniometer. The azimuthal angle, ϕ, at 90° corresponds to the draw direction, and $\phi = 0°$ corresponds to the transverse directions of the sample. Monochromatic Cu Kα beam was generated with a nickel filter at 40 kV and 35 mA. Azimuthal intensities were also scanned at the tail ends of the 010 peak at $2\theta = 13.8°$ and 17.6° for background correction. Background intensity at 15.4° was obtained by interpolating the data from these two azimuthal scans. The average cosine square angle $\langle \cos^2 \phi_{010,Z} \rangle$ the normal of (010) plane made with the draw direction, *Z*, was calculated

10.1021/ma010317z CCC: $20.00
Published on Web 08/24/2001

from the corrected azimuthal intensities, $I(\phi)$, as follows:

$$\langle \cos^2 \phi_{010,Z} \rangle = \frac{\int_0^{\pi/2} I(\phi) \sin \phi \cos^2 \phi \, d\phi}{\int_0^{\pi/2} I(\phi) \sin \phi \, d\phi} \quad (1)$$

The average square cosine angle $\langle \cos^2 \phi_{c,Z} \rangle$ of PTT *c*-chain axis made with the draw direction is given by

$$\langle \cos^2 \phi_{c,Z} \rangle = 1 - 2\langle \cos^2 \phi_{010,Z} \rangle \quad (2)$$

This equation was based on Wilchinsky's treatment of uniaxial orientation.[10] Details of the symmetry conditions used to derive eq 2 had been described in a separate publication.[11] The crystal orientation function is calculated from the Herman orientation equation:

$$f_c = \frac{3\langle \cos^2 \phi_{c,Z} \rangle - 1}{2} \quad (3)$$

For random orientation, $f_c = 0$. When the chains are perfectly oriented parallel and perpendicular to the draw direction, $f_c = 1$ and -0.5, respectively.

Polarized ATR-IR Dichroic Ratio Measurements. Polarized attenuated total reflectance (ATR) IR spectra were obtained with a Nicolet 20 DXB FTIR spectrometer using a Harrick Seagull accessory with a rotatable ATR sample holder. The number of scans was 128. The spectral resolution was 2 cm^{-1}. Spectra obtained by the ATR method were often modified to some degrees depending on how good is the contact between the sample surface and ATR crystal. Transmission spectra using thin films would eliminate this problem; however, the same thin film would give too weak WAXD intensity for crystal orientation and transition moment measurements in this work. To ensure good contact between the sample and ATR crystal, Wall's method[12] was followed. The ATR crystal and sample were clamped with a clamping torque of 0.71 N m for reproducibility.

Polarized spectra were obtained at 50° incident angle with electric polarization parallel and perpendicular to the draw direction. Galactic Industries programs Spectra-Calc and Grams were used to process spectra, baseline correction and to normalize absorbance. Since the 1410 cm^{-1} intensity did not change with annealing and drawing, it was used as an internal reference band. The dichroic ratio, R, was obtained from the ratio of absorbances with the electric vector parallel, $A_{\parallel}$, and perpendicular, $A_{\perp}$, to the draw direction:

$$R = \frac{A_{\parallel}}{A_{\perp}} \quad (4)$$

For each vibration mode R of the undrawn sample was checked to ensure the methodology, and the choice of reference band gave $R = 1.0 \pm 0.1$.

Assuming cylindrical symmetry for uniaxial orientation, the "isotropic" absorbance, A_{avg} was obtained by averaging $A_{\parallel}$ and $A_{\perp}$ as

$$A_{avg} = (A_{\parallel} + 2A_{\perp})/3 \quad (5)$$

Alternatively, individual normal and in-plane $A_{\perp}$ could be measured by rotating the polarizer and sample by 90°. However, analysis of absorbances obtained this way requires knowledge of the spatial attenuation indices and refractive indices, n, along the three principal directions.[13,14] Since n for each principal direction changes with draw and are impractical to track, an average n value is assumed to calculate the attenuation indices and structure factors. Lee et al.[15] noted the error involved with this assumption was small. Walls[12] also discussed the difficulties of anisotropic effect on the refractive indices in PET orientation study. This more rigorous treatment is necessary for biaxial orientation where there are large differences between in-plane and normal transverse absorbances. In this uniaxial orientation study, we used the simpler averaging method according to eq 5.

Vibration modes used in this study were the 811 and 933 cm^{-1} CH_2 rocking, 1037 cm^{-1} gauche C−C glycol residue stretching, 1173 cm^{-1} benzene ring in-plane C−H stretching, 1358 and 1385 cm^{-1} CH_2 wagging, and 1505 cm^{-1} benzene ring in plane C−C stretching bands.

Crystallinity Measurements. Crystallinity was measured from density using a Fischer 1 L density gradient column using a mixture of sodium bromide solutions. Lab Glass density beads with accuracy to three decimal points in the range 1.210−1.360 were used for calibration. The weight fraction crystallinity, X_c, was calculated from

$$X_c = \frac{\rho_c(\rho - \rho_a)}{\rho(\rho_c - \rho_a)} \quad (6)$$

where ρ is the density of the sample. The density of a 100% crystalline PTT, ρ_c, calculated from unit cell dimensions given by Desborough et al.[4] was 1.432 g/cm^3; the density of 100% amorphous PTT, ρ_a, calculated by the group contribution method using molar volumes given by Van Krevelen,[16] was 1.295 g/cm^3.

Results and Discussion

Drawing Behavior. A polymer is capable of drawing if its true stress−strain curve satisfies the Considère criterion such that two tangents could be drawn from the origin at draw ratio = 0 to the curve.[17] Such polymer can then neck and draw. For a glassy, brittle polymer the above condition could be met when it is heated to a sufficiently high temperature above its glass transition temperature, T_g. Therefore, it is a practice to heat a polymer to above T_g and usually to a much higher temperature for drawing. Heating lowers the yield and drawing stresses and increases the polymer's drawability for achieving a high draw ratio.

Figure 2 shows the stress−strain curves of PTT at various draw temperatures. At room temperature PTT is ductile. It yields at 5.4% strain cold draws with a natural draw ratio of about 3.2, then strain-hardens, and breaks at 360% strain. At 35 °C, still below T_g, the yield and drawing stresses decrease to 30 and 17.2 MPa, respectively, and the strain at break increases to 475%. At 50 °C, just above T_g, PTT becomes rubbery. The Young's modulus decreases by about 2 orders of magnitude from a room temperature modulus of 1140 MPa to 12.9 MPa, and the overall drawability increases with a strain at break of nearly 600%. However, when the draw temperature was increased to 75 °C, just 30 °C above T_g, instead of becoming more rubbery and capable of higher draw, PTT became ductile again. The modulus unexpectedly increased by more than 10-fold to 189 MPa. The overall drawability decreased with a drop in breaking strain to 390%. In fact, the 75 °C stress−strain curve looked similar to that of room temperature. Instead of higher draw with increasing temperature, PTT draw first increased, went through a maximum, and decreased, all happening over a narrow range of temperature from room temperature to T_g + 30 °C.

When PTT was annealed at 90 °C for 3 min, it became brittle. The room temperature breaking strain was only ∼10%, and it could not be drawn at all compared to the starting polymer. To draw this annealed brittle PTT, the polymer had to be heated to a high temperature of >140 °C. Thus, there is a range of temperatures, approximately between 80 and 140 °C, depending on the

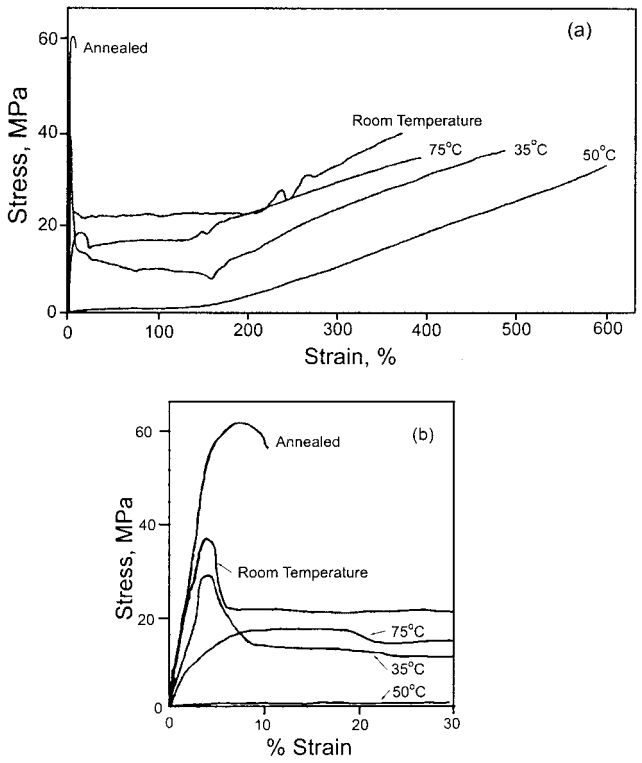

Figure 2. (a) Stress−strain curves of PTT at room temperature, 35, 50, and 75 °C and of an annealed PTT. (b) Enlarged portion of the curves from 0 to 30% strain.

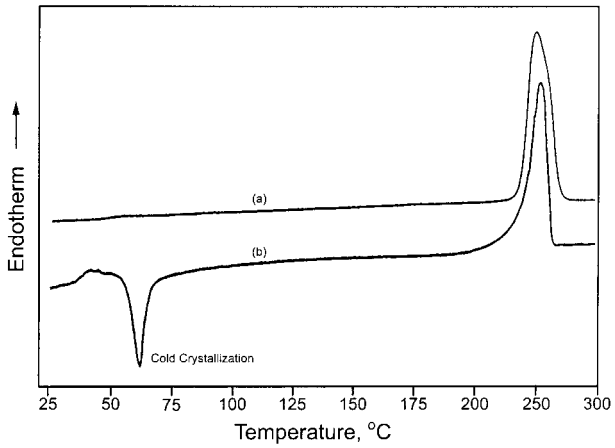

Figure 3. Differential scanning calorimetric scans of (a) a slowly cooled and (b) a quenched PTT.

polymer's prior thermal history, starting morphology, crystallinity, and the duration at the draw temperature, where heating is detrimental to PTT drawing.

The observed change in draw ratio going through a maximum is similar to the stress−strain failure envelope found in elastomers and amorphous polymers. The draw ratio also goes through a maximum with temperature or strain rate. Because of the superposition between temperature and strain rate, the fracture process is dominated by viscoelastic effects.[17] In the case of PTT, the behavior could be explained by its thermal behavior and crystallization kinetics during draw. Figure 3 shows the differential scanning calorimetry (DSC) scans of a slowly cooled (10 °C/min) and a rapidly quenched (150 °C/min) PTT. T_g and peak melting point are 45 and 228 °C, respectively. When PTT is heated, the quenched sample begins to cold crystallize at about 50 °C with a peak temperature of 65 °C whereas the slowly cooled sample did not. Chuah[18] compared the isothermal crystallization kinetics of PET, PTT, and PBT and found PTT to crystallize at a rate in between those of PET and PBT. PTT's Avrami rate constants were about an order of magnitude faster than PET and an order of magnitude slower than PBT at the same degree of undercooling. Bulkin et al.[19] found when PTT film was heated, the crystallinity increased at a much faster rate than PET in the rapid scanning Raman spectroscopy crystallization kinetic study. At 71 °C, PTT crystallinity reached 80% of its equilibrium value in <1 min while PET did not crystallize at all.

PET is well-known to crystallize very slowly while PBT has a very fast crystallization rate.[20] With these two extremes, melt-processed PET is generally quite amorphous with <5% crystallinity while PBT tends to be highly crystalline with crystallinity as high as ∼50%. With an intermediate crystallization rate PTT could have a broad range of morphology and crystallinity depending on the crystallization conditions as shown by the two examples in the DSC curves (Figure 3).

When PTT's initial morphology has a low degree of crystallinity, it cold crystallizes during hot drawing. The rate and extent of cold crystallization depend on its initial degree of crystallinity and the drawing temperature. Thus, there are two opposing events occurring during PTT hot drawing. The elevated temperature softens the polymer aiding drawing while the onset of cold crystallization stiffens the polymer and reduces drawing. The net result is a maximum in PTT draw ratio as a function of draw temperature. When cold crystallization is fast and is the dominating event, PTT's crystallinity increases rapidly so that the polymer changes from being ductile to brittle during drawing and in some cases becomes too brittle to draw. When this happens, the only recourse is to increase the draw temperature by a large step to >140 °C to further soften the polymer for drawing.

Orientation Development in Tensile Drawing. a. Wide-Angle X-ray Diffraction Orientation. PTT crystal is triclinic.[4,5,21,22] The *c*-axis contains two repeating units, and the methylene groups are arranged in highly contracted gauche−gauche conformations. Because of low crystal symmetry, as many as six WAXD reflections may be needed to measure f_c of polymer with triclinic cell[23] unless it has a suitable 00*l* reflection. PTT does have a 002 reflection, but it is tilted about 3° away from the meridian. It thus forms two off-meridian reflections. However, they are too close to each other that they appear as a single meridianal reflection. Unlike PET with a well-resolved off-meridian $\bar{1}50$ reflection,[24] PTT's 002 off-meridian reflection cannot be resolved easily even at high orientation. It is therefore better to use the strong 010 equatorial reflection for orientation function measurement. Because of the fortuitous coincidence of PTT's β-angle = 90°, its reciprocal *b**-axis is orthogonal to both *a*- and *c*-axis. Chuah and Chang[11] showed, by using this orthogonal relationship and applying cylindrical symmetry around the *Z*-uniaxial draw direction, Wilchinsky's equation can be reduced into a simple form given by eq 2.

Table 1 shows changes in PTT WAXD f_c, densities, and crystallinities drawn at 50 and 75 °C. f_c increased rapidly with draw and reached 0.79 at a moderate draw ratio of 2.8. This corresponded to an average angle of 39° the polymer's chains made with the draw direction. f_c saturated at about 0.96 at higher draw. At 75 °C,

Table 1. Changes in WAXD Orientation Function f_c, Density, % Crystallinity as a Function of Draw Ratio, and the Transition Moment Angles of Crystalline IR Bands

				IR bands transition moment angle, ψ (deg)		
draw ratio	ρ, g/cm^3	% X_c	f_c	933 cm^{-1}	1358 cm^{-1}	1505 cm^{-1}
			Draw Temperature: 50 °C			
1	1.311	13.0				
1.9	1.314	15.4				
2.8	1.324	23.4	0.790	54	30	48
3.5	1.327	25.7	0.902	54	29	46
4	1.329	27.3	0.965	54	28	44
			Draw Temperature: 75 °C			
2.6	1.332	29.6	0.598	54	29	44
3.3	1.332	29.6	0.885	54	29	43
				av 54	av 29	av 45

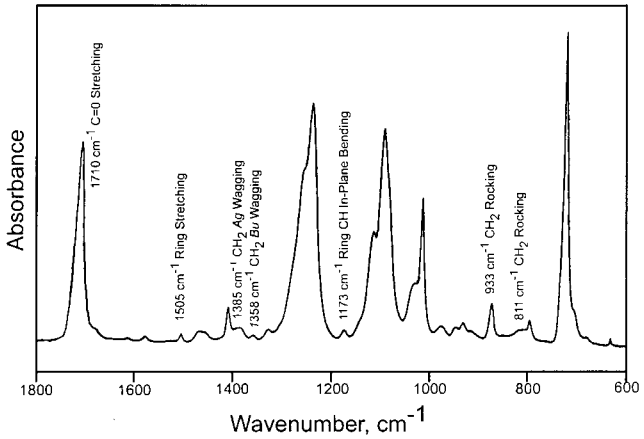

Figure 4. IR spectra of PTT with identified bands used in the study.

orientation development is lower than at 50 °C; however, the drawn samples have higher crystallinities. Besides strain-induced crystallization, drawing at 75 °C was accompanied by a substantial amount of simultaneous cold crystallization. The increase in PTT crystal orientation function with draw is very similar to that of PET[25] and other semicrystalline polymers.[26]

b. IR Dichroism. Figure 4 shows the IR spectra of an unoriented PTT. Before discussing PTT IR dichroism, it is instructive to examine the assigned bands whether they are from crystalline or amorphous phase and whether they are associated with the trans (*t*) or gauche (*g*) conformation. Ward and Wilding[27] compared in details the IR and Raman spectra of PET, PTT, and PBT. Particular attention was given to changes in the spectra before and after annealing. Vibration modes with increased intensity after annealing were assigned to the crystalline region. They found the spectra to be essentially the same for the three polyesters but with significant differences in the regions around 900, 1400, and 1100 cm^{-1}.

The 1358 and 1385 cm^{-1} bands were assigned to CH_2 wagging. In an IR study of PTT uniaxial and biaxial film drawing, Lee et al.[15] attributed them to the trans and gauche conformers, respectively. However, Ward and Wilding[27] found the band intensities increased on crystallization, and they were also present in the Raman spectrum of annealed PTT. Bulkin et al.[19] also found the 1358 cm^{-1} intensity to increase after annealing and used it to study PTT crystallization kinetic study. Thus, the 1358 cm^{-1} CH_2 wagging must be from the crystalline region. Since PTT's three methylene groups are arranged in a *gg* conformation in the crystal, the 1358 cm^{-1} CH_2 wagging is therefore associated with the crystalline phase gauche conformers and not the trans conformers. The CH_2 wagging band assignments to the crystalline and amorphous phases are just the opposite of PET.

Table 2. PTT IR Band Assignments

wavenumber, cm^{-1}	assignment	phase
811	CH_2 rocking of glycol residue	amorphous
933	CH_2 rocking of glycol residue	crystalline[19] amorphous[27]
1037	*Ag* C−C stretchig	crystalline
1173	ring *Ag* in-plane C−H bending	amorphous[19]
1358	*Bu* CH_2 wagging	crystalline
1385	*Ag* CH_2 wagging	amorphous
1505	benzene ring C−C stretch	crystalline
1710	*Bu* C=O stretch	

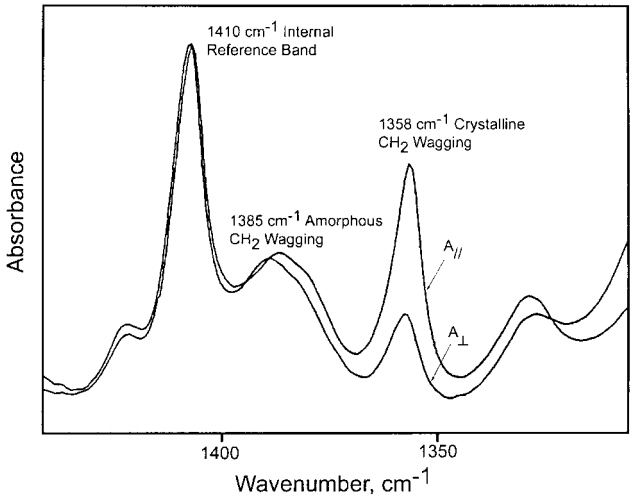

Figure 5. IR spectra of parallel and perpendicularly polarized 1358 and 1385 cm^{-1} CH_2 stretching bands. The 1410 cm^{-1} band was used as an internal reference band.

Table 2 summarized the vibration modes used in this study. Unless otherwise referenced, the assignments were based on Ward and Wilding.[27] Crystalline phase assignment was based on the substantial increase in band intensity after annealing; trans conformers were deduced from them being excluded in the crystalline phase and therefore can occur only in the amorphous phase.

Figures 5 and 6 show the polarized spectra of drawn PTT and the changes in 1358 and 1385 cm^{-1} dichroic ratios as a function of draw, respectively. The 1358 cm^{-1} band was very sensitive to draw while the 1385 cm^{-1} band was not. The latter dichroic ratio increased only slightly with draw and was <1.4 even at the highest draw compared to about 7 for 1358 cm^{-1}. The next two dichroic sensitive bands are the 1037 cm^{-1} gauche C−C stretch of the glycol residue and the 1505 cm^{-1} benzene ring C−C stretch (Figure 7). The increase in dichroic ratios with draw of the 1505 cm^{-1} band is, however, much smaller compared to the 1037 cm^{-1} band. The fitted lines are for the 50 °C draw. For both bands, the 75 °C dichroic ratios were significantly higher than at 50 °C for equivalent draw although WAXD measurements gave lower crystal orientations (Table 1). Although these are puzzling, there were not enough 75 °C data to make any conjecture.

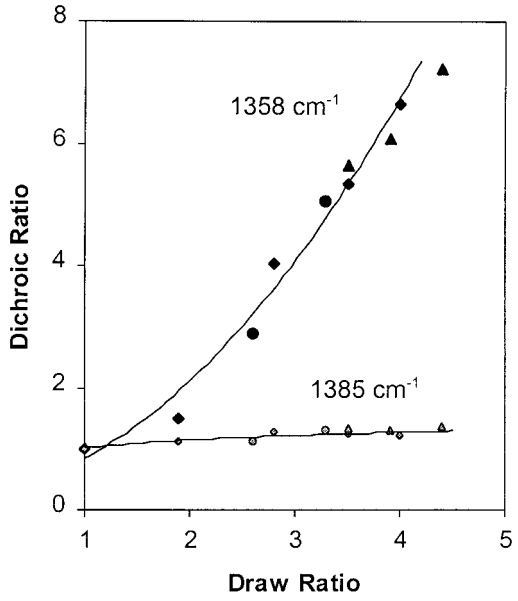

Figure 6. IR dichroic ratios of 1358 and 1385 cm^{-1} bands as a function of draw ratio. Draw temperatures: 35 (▲), 50 (◆), and 75 °C (●). The 1385 cm^{-1} data have the same legends but with smaller markers.

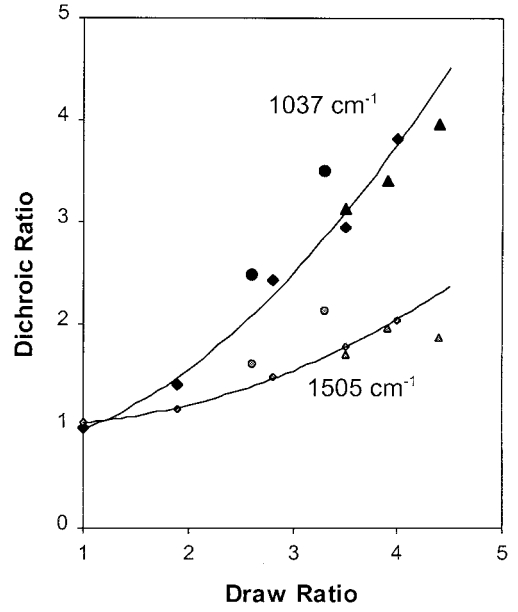

Figure 7. IR dichroic ratios of 1037 and 1505 cm^{-1} bands as a function of draw ratio. Draw temperatures: 35 (▲), 50 (◆), and 75 °C (●). The 1505 cm^{-1} data have the same legends but with smaller markers.

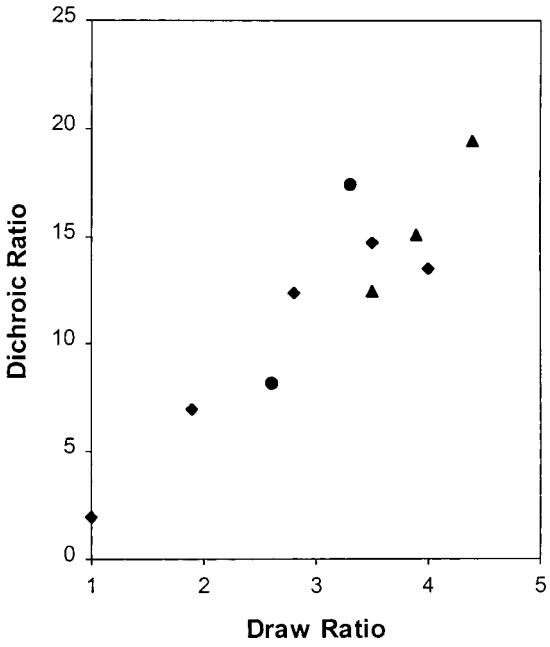

Figure 8. IR dichroic ratios of 933 cm^{-1} CH_2 rocking band as a function of draw ratio. Draw temperatures: 35 (▲), 50 (◆), and 75 °C (●).

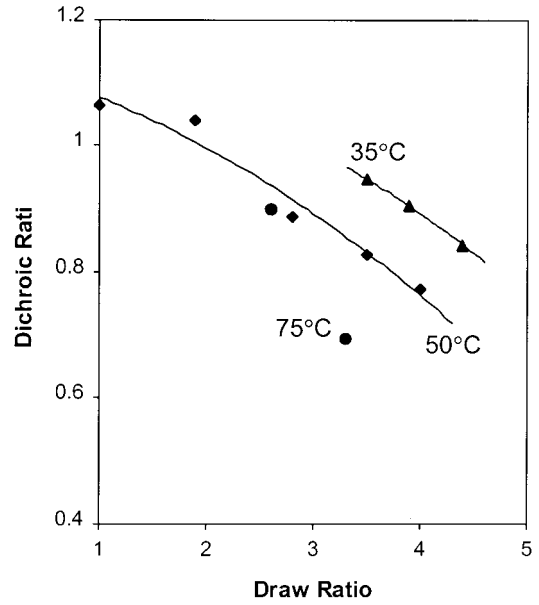

Figure 9. IR dichroic ratios of 1173 cm^{-1} band as a function of draw ratio. Draw temperatures: 35 (▲), 50 (◆), and 75 °C (●).

Ward and Wilding[27] assigned both 933 and 811 cm^{-1} bands to the amorphous CH_2 rocking of the glycol residue. However, Bulkin et al.[19] found the 933 cm^{-1} band intensity increased after annealing and assigned it to crystalline phase CH_2 rocking. In our study this vibration mode was the most sensitive to drawing with a large increase in the dichroic ratio (Figure 8). The isotropic intensity obtained by eq 5 also correlated with increased crystallinity supporting a crystalline band assignment. The amorphous 1173 cm^{-1} in plane ring C−H stretching showed weak dirchroism, and its intensity was found to decrease by about 40% upon annealing.[19] The decrease in the dichroic ratio appeared to be sensitive to draw temperatures (Figure 9). For each draw temperature, the 1173 cm^{-1} dichroic ratios showed different decreasing trends albeit the limited number of samples compared to Figure 6, where all 1358 cm^{-1} dichroic ratios from the three draw temperatures fell onto a single curve. The 1720 cm^{-1} C═O stretching is made up of a complex group of bands because of the nonplanar nature of the terephthaloyl residue.[27] We found it to have low dichroism.

Transition Moments of Crystalline Phase Vibrating Modes. The dichroic ratio is a useful parameter for assessing the degree of chain orientation. It is related to the Herman orientation function[28] by

$$f_c = \frac{(R-1)(R_0+2)}{(R_0-1)(R+2)} \tag{7}$$

where R_0 is the dichroic ratio of sample with perfect chain alignment in the draw direction, given by

$$R_0 = 2 \cot^2 \psi \tag{8}$$

ψ is the angle between the transition moment vector and the chain axis. It is often assumed to be either parallel to or perpendicular to the chain axis. Although the transition moment of polyethylene's 1894 cm^{-1} CH_2 rocking mode is listed as perpendicular to the *c*-axis, Desper[29] showed it made an angle of about 39° with the *a*-axis. Similarly, Samuels[30] obtained a 72° angle for polypropylene's 1220 cm^{-1} CH_2 wagging transition moment vector.

By combining WAXD f_c and IR dichroic measurements, ψ angles for three PTT crystalline 933, 1358, and 1505 cm^{-1} vibration modes were found to be 54°, 29°, and 45°, respectively (Table 1). To make sure that these bands are of crystalline origin, otherwise the transition moment determination using WAXD f_c would become meaningless, we checked whether their intensities increased with sample crystallinities after drawing. The average intensities obtained according to eq 5 of both 933 and 1358 cm^{-1} vibrations tracked well with the increase in sample crystallinities; however, the increase of the 1505 cm^{-1} intensity was small and scattered. Although this band was assigned by Ward and Wilding[27] to be a crystalline benzene C−C stretch and was dichroic sensitive to draw, due to the poor correlation of its intensity with crystallinty, the ψ angle of the 1505 cm^{-1} band is reported with reservation, pending a more precise phase assignment. The 1037 cm^{-1} band, though, showed strong dichroism with draw and was assigned as a crystalline band;[27] the average intensities did not correlate with the increase of crystallinities in this study. The crystalline assignment is therefore suspect, and its transition moment was not reported.

In the PTT triclinic cell, the chains are arranged zigzag with each of the two repeating units inclined in opposite direction at an angle of about 52° to the *c*-axis.[4] Since the center of the benzene unit is set at the origin of the cell, the 1505 cm^{-1} benzene C−C stretch would have a transition moment in the direction of the setting angle. The experimental ψ angle of 45° is in good agreement with the expected transition moment direction albeit the uncertainty in the assignment of the 1505 cm^{-1} band to the crystalline phase.

The comparisons of the 933 cm^{-1} CH_2 rocking and 1358 cm^{-1} CH_2 wagging ψ angles to the spatial arrangement of the three gauche−gauche methylene units are more difficult to visualize. With a ψ angle of 54°, the average transition moment vector of CH_2 wagging coincides with the chain direction, which is tilted about 52° from the *c*-axis. Since the transition moment of CH_2 rocking mode is orthogonal to that of CH_2 wagging, considering a ψ angle of 29° tilted from the *c*-axis away from that of CH_2 wagging, the two transition moments are nearly orthogonal to each other within experimental error.

Since all three bands showed moderate to large increase in dichroic ratio with drawing, knowledge of the transition moment angles and dichroic ratio with draw and with known transition moment angles IR dichroism can be used as an alternate method to measure the PTT crystal orientation function.

Conformational Changes in Drawing. With a highly compliant crystal and gauche methylene conformations, an interesting question to ask is whether PTT crystal undergoes transformation to an all-trans crystal form like PBT when it is stretched.[31] Poulin-Dandurand et al.[5] had calculated the PTT conformational energy in the crystal and showed an all-trans conformation has too high conformational energy and is unstable. Early work by Jakeways et al.[3] showed PTT crystal fiber period increased by about 7% when the fiber is stretched with 10% strain because of the low crystal modulus. Since the force to rotate C−C bond is low, their results suggested the gauche methylene units could possibly rotate by a substantially large angle toward trans under strain. In an in situ WAXD fiber deformation study with synchrotron radiation, Wu et al.[32] found PTT 002 *d* spacing increased with applied strain similar to Jakeways et al.'s observation. However, they were able to stretch the fiber period from 18.3 to 20.6 Å, an increase in the *c*-axis length by ∼25%. The extended fiber period was close to the length of an all-trans methylene conformation. The *b*-axis 010 *d*-spacing decreased correspondingly. When the strain was further increased beyond this maximum *c*-axis length, the fiber period reverted almost immediately to near its original length. The stretched trans conformation, if it existed, occurred temporally under strain. Thus, there was a critical lattice strain on how much the fiber period can be stretched, above which the crystal reverted back to the lower energy conformation. It is, however, not clear how this was achieved.

Although there were no simultaneous spectroscopic measurements to confirm the chain conformation, the highly compliant PTT crystal and the early deformation studies[3,8] suggested a likely *gg* → *tt* transformation similar to the strain-induced reversible PBT *gtg* α− → *ttt* γ-crystal transformation.[33] If confirmed, it would be the first report of an alternate PTT crystal form. Another possible explanation for the observed increase in fiber period under strain is the chain which was originally set at 52° angle from the *c*-axis, tilted to a lower angle with applied strain, resulted in an increase of the *c*-axis length. Since the force required for chain rotation is low, any chain tilting would have to be preceded or accompanied by C−C bond torsional rotation; tilting of the chain is unlikely to occur as an independent event. The question of PTT chain conformation under strain remains an interesting topic for future study.

We examined the effect of drawing on PTT conformational changes using selected IR bands. PET has two well-established trans 1340 cm^{-1} and gauche 1370 cm^{-1} bands. Walls[12] found the 1340 cm^{-1} band intensity increased with uniaxial drawing and saturated when the draw ratio was above 3. This was accompanied by a simultaneous decreased in the 1370 cm^{-1} intensity. The changes were associated with stress-induced crystallization during draw, converting the gauche conformers in the amorphous phase to the extended trans species either in the amorphous phase or into the crystalline phase. Similar changes in these two band intensities were also observed during the physical aging and annealing[34,35] of PET.

Intensities of PTT's 1358 and 1385 cm^{-1} bands also showed similar changes in intensities after drawing and correlated to changes in sample crystallinities (Figure 10). However, the correlation with crystallinity was poor compared to PET's 1340 and 1370 cm^{-1} bands.[34]

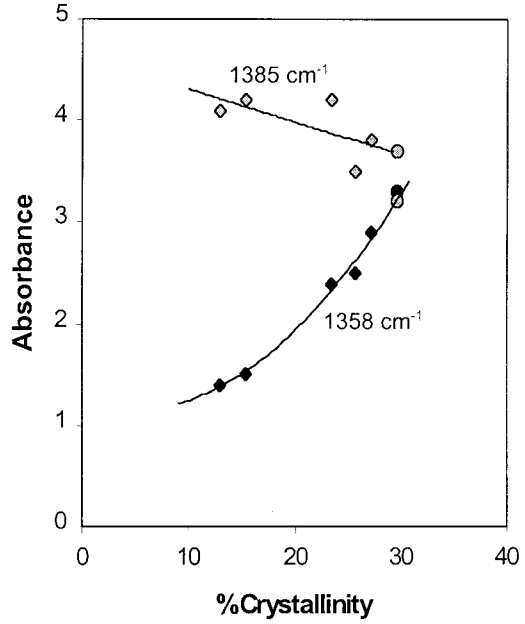

Figure 10. Average absorbance of 1358 and 1385 cm^{-1} bands as a function of crystallinity after drawing. Draw temperature: 50 (◆) and 75 °C (●). Filled markers are for 1358 cm^{-1} bands, and shaded markers are for 1385 cm^{-1} bands.

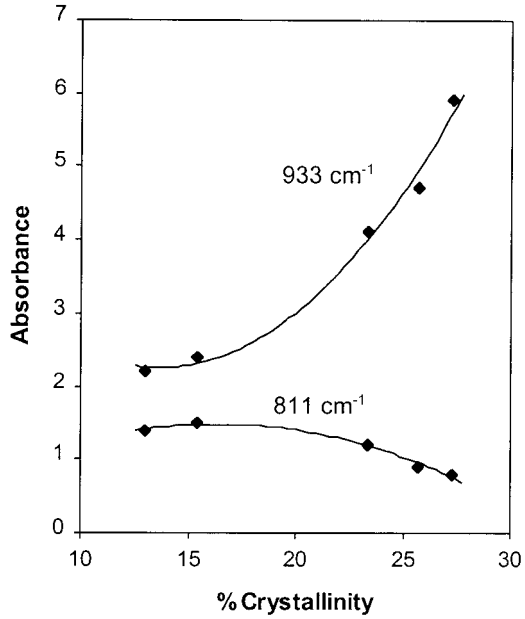

Figure 11. Averaged absorbance of 933 and 811 cm^{-1} bands as a function of crystallinity. Draw temperature: 50 °C.

On examining the 933 and 811 cm^{-1} CH_2 rocking bands, we found similar changes in intensities (Figure 11). The 933 cm^{-1} band had been assigned to crystalline region by Bulkin et al.[19] and is of a gauche conformer. Our results supported the assignment. Figure 11 shows the 933 cm^{-1} intensity increases and the 817 cm^{-1} intensity simultaneously decreases as a function of crystallinity. The plot of the intensities as a function of draw ratio also showed similar trends. Since trans conformers are unstable in the crystalline region, they could exist only in the amorphous phase; the corresponding decrease of the 811 cm^{-1} intensity with crystallinity suggests it is an amorphous trans conformer, being incorporated into the crystalline phase through strain-induced or cold crystallizations. We thus used these two bands to estimate PTT conformational

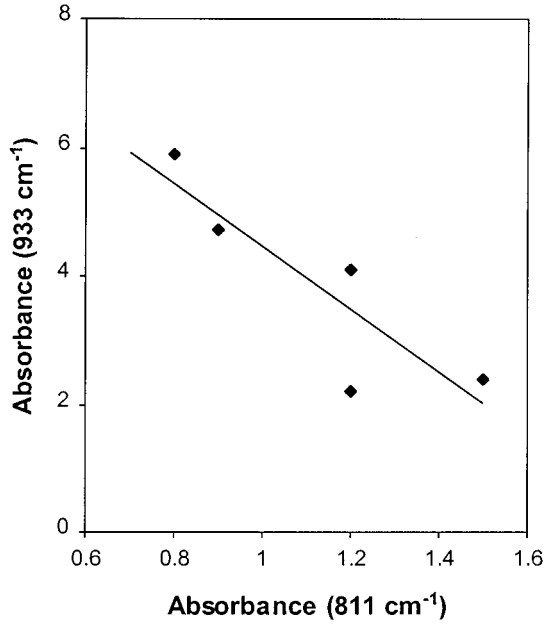

Figure 12. Correlation between 933 and 811 cm^{-1} absorbances.

changes in tensile drawing. By plotting the respective intensity pairs of these two bands (Figure 12), the 933 cm^{-1} intensity, A_{933}, was found to be 4.9 times stronger than the 811 cm^{-1} intensity, A_{811}. Assuming a two-phase model, the gauche content in drawn PTT is estimated by

$$\text{gauche content} = \frac{A_{933}}{A_{933} + 4.9A_{811}} \qquad (9)$$

It is noteworthy that a two-phase assumption may not adequately described PTT. Our solid-state ^{13}C NMR crystalline/amorphous phase study[36] required three spin−lattice relaxation decays for curve fitting, suggesting there might be a third undetermined phase besides the conventional crystalline/amoprhous phase. For PET various studies[37,38] showed the presence of a third rigid amorphous phase, which could likely exist in PTT. For the purpose of gaining insight into PTT drawing behavior, a simple two-phase model is assumed to show the trend of conformational changes.

Figure 13 shows the gauche content increases gradually with draw at 50 °C drawing temperature; however, the 35 and 75 °C data were scattered. The two 75 °C data were particularly way off. When the gauche content was plotted against sample crystallinity (the 35 °C crystallinities were not measured, and the decade old samples were no longer available for measurements), the scatters disappeared (Figure 14). Unlike Wall's study[12] where the increase in PET's total trans content came from only stress-induced crystallization, PTT's gauche content is dependent on the sample's final crystallinity gained from a combination of strain-induced crystallization from drawing and from draw temperature-dependent cold crystallization. The relative contribution of these crystallization mechanisms to the increase in crystallinity is different at each draw temperature; the increase of gauche content with draw ratio is unique to each draw temperature like the 50 °C draw of Figure 13. It is, however, directly related to sample final crystallinity irrespective of the draw conditions.

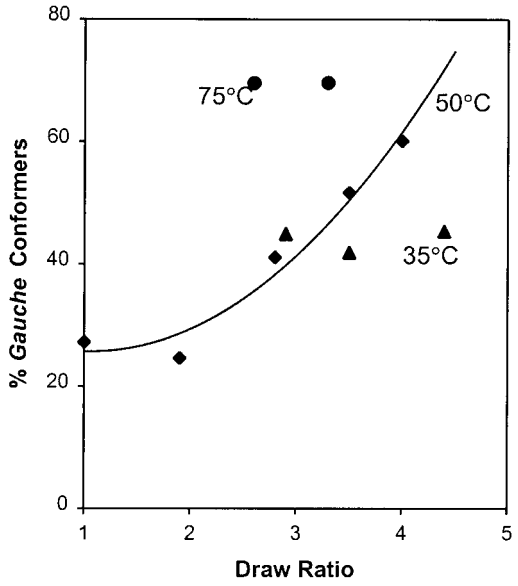

Figure 13. Increase in % PTT gauche content as a function of draw ratio. Draw temperatures: 35 (▲), 50 (◆), and 75 °C (●).

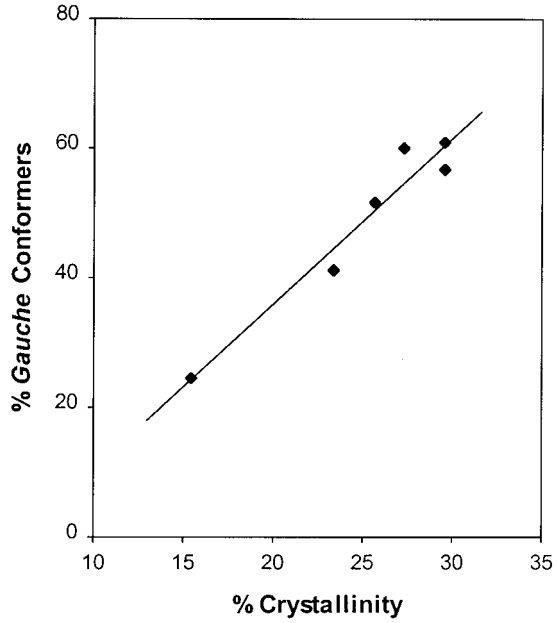

Figure 14. Percent gauche content as a function of wt % crystallinity for PTT drawn at 35, 50, and 75 °C and to various draw ratios of Figure 13.

Conclusions

Tensile drawing of PTT was studied as a function of temperature above and below its T_g. Instead of a typical increase in draw ratio with increasing temperature, the PTT draw ratio first increased, went through a maximum, and decreased, all occurring within a narrow range of temperature between T_g and $T_g + 30$ °C. The mechanism of this phenomenon is different from the viscoelastic effect on the stress−strain failure envelope found in elastomers, and amorphous polymer PTT's draw behavior was caused by the onset of cold crystallization during drawing, which caused in situ morphological changes giving PTT a rubbery, ductile, or brittle behavior during the drawing process. When cold crystallization became the predominating event, it led to ductile−brittle transition during drawing and caused draw breaks. The crystal orientation function measured by WAXD increased rapidly with draw and saturated at $f_c \cong 0.96$ when drawn at 35, 50, and 75 °C. The 933, 1037, 1358, and 1505 cm^{-1} vibration modes showed strong IR dichroism and are sensitive for orientation characterization. By combining WAXD measured f_c and IR dichroic measurements, the transition moment vectors of the crystalline 933, 1358, and 1505 cm^{-1} vibrations were found to make 54°, 29°, and 45° angles to the *c*-chain axis. The 933 and 811 cm^{-1} CH_2 rocking modes were assigned to gauche and trans conformers, respectively, and were used to measure gauche conformational changes in drawing. The gauche content was found to depend uniquely on the final crystallinity resulted from a combination of strain-induced crystallization from drawing and cold crystallization at the elevated draw temperature.

Acknowledgment. The author thanks Benjamin Chang, Clarke Champie, Janusz Grebowicz, Russ Vinson, and John Webb of Shell Chemical Company and Jing Wu and Jerry Schultz of University of Delaware for help in experimental work and discussions.

References and Notes

(1) Chuah, H. H.; Brown, H. S.; Dalton, P. A. *Int. Fiber J.* **1963**, *10* (5), 50.
(2) Ward, I. M.; Wilding, M. A.; Brody, H. *J. Polym. Sci., Polym. Phys. Ed.* **1976**, *14*, 263.
(3) Jakeways, R.; Ward, I. M.; Wilding, M. A.; Desborough, I. J.; Pass, M. G. *J. Polym. Sci., Polym. Phys. Ed.* **1975**, *13*, 799.
(4) Desborough, I. J.; Hall, I. H.; Neisser, J. Z. *Polymer* **1979**, *20*, 545.
(5) Poulin-Dandurand, S.; Perex, S.; Revol, J.-F.; Brisse, F. *Polymer* **1979**, *20*, 419.
(6) Mencik, Z. *J. Polym. Sci., Polym. Phys. Ed.* **1975**, *13*, 2173.
(7) Gedde, U. W. *Polymer Physics*; Chapman & Hall: New York, 1995.
(8) Nakamae, K.; Nishio, T.; Hata, K.; Yokoyama, F.; Matsumoto, T. *Zairyo* **1986**, *35*, 1066.
(9) Sakurada, I.; Kani, K. *J. Polym. Sci., Part C* **1970**, *31*, 57.
(10) Wilchinsky, Z. *Advances in X-Ray Analysis*; Plenum Press: New York, 1963; Vol. 6, p 231.
(11) Chuah, H. H.; Chang, B. T. A. *Polym. Bull.* **2001**, *46*, 307.
(12) Walls, D. R. *Appl. Spectrosc.* **1991**, *45*, 1193.
(13) Koenig, J. L.; Cornell, S. W.; Witenhafer, D. E. *J. Polym. Sci., Part A-2* **1967**, *5*, 301.
(14) Hobbs, J. P.; Sung, C. S. P.; Krishnan, K.; Hill, S. *Macromolecules* **1983**, *16*, 193.
(15) Lee, H. S.; Park, S. C.; Kim, Y. H. *Macromolecules* **2000**, *33*, 7994.
(16) Van Krevelen, D. W. *Properties of Polymers*, 2nd ed.; Elsevier: Amsterdam, 1976; pp 51−62.
(17) Ward, I. M. *Mechanical Properties of Polymers*; John Wiley & Sons: New York, 1969.
(18) Chuah, H. H. *Polym. Eng. Sci.* **2001**, *41*, 308.
(19) Bulkin, B. J.; Lewin, M.; Kim, J. *Macromolecules* **1987**, *20*, 830.
(20) Brydson, J. A. *Plastic Materials*, 5th ed.; Butterworths: London, 1989.
(21) Chatani, Y.; Higashibata, N.; Takase, M.; Tadokoro, H.; Hirahara, T. *Ann. Meet. Soc. Polym. Sci., Kyoto, Prepr.* **1977**, 427.
(22) Moss, B.; Dorset, D. L. *J. Polym. Sci., Polym. Phys. Ed.* **1982**, *20*, 1789.
(23) Alexander, L. E. *X-Ray Diffraction Methods in Polymer Science*; John Wiley & Sons: New York, 1969.
(24) Dumbleton, J. D.; Bowles, R. *J. Polym. Sci., Part A-2* **1966**, *4*, 951.
(25) Ward, I. M. *J. Text. Inst.* **1995**, *86*, 289.
(26) Wilchinsky, Z. W. *Polymer* **1964**, *5*, 271.
(27) Ward, I. M.; Wilding, M. A. *Polymer* **1977**, *18*, 327.
(28) Jasse, B.; Koenig, J. L. *Rev. Macromol. Chem.* **1979**, *C17*, 61.

(29) Desper, C. R. *J. Appl. Polym. Sci.* **1969**, *13*, 168.
(30) Samuels, R. J. *Structured Polymer Properties*; John Wiley & Sons: New York, 1974.
(31) Jakeways, R.; Smith, T.; Ward, I. M.; Wilding, M. A. *J. Polym. Sci., Polym. Lett. Ed.* **1976**, *14*, 42.
(32) Wu, J.; Schultz, J. M.; Samon, J.; Pangelinan, A.; Chuah, H. H. *Polymer* **2001** *42*, 7141.
(33) Hall, I. M.; Pass, M. G. *Polymer* **1976**, *17*, 807.
(34) Qian, R.; Shen, D.; Sun, F. *Macromol. Chem. Phys.* **1996**, *197*, 1485.
(35) Wang, Y.; Lu, J.; Shen, D. *Polym. J.* **2000**, *32*, 560.
(36) Haddix, G. W.; Chuah, H. H. Quantification of the Crystalline Fraction of Poly(Propylene Terephthalate) Using 13C Solid-State NMR. Technical Progress Report WRC 191-92, Shell Chemical Company, 1992.
(37) Bianchi, R.; Di Dino, G. *Macromolecules* **1992**, *25*, 2490.
(38) Fu, Y.; Busing, W. R.; Jin, Y.; Affholter, K. A.; Wunderlich, B. *Macromolecules* **1993**, *26*, 2187.

MA010317Z